Improving the virtual source method by wavefield separation

Kurang Mehta[1], Andrey Bakulin[2], Jonathan Sheiman[2], Rodney Calvert[2], and Roel Snieder[1]

ABSTRACT

The virtual source method has recently been proposed to image and monitor below complex and time-varying overburden. The method requires surface shooting recorded at downhole receivers placed below the distorting or changing part of the overburden. Redatuming with the measured Green's function allows the reconstruction of a complete downhole survey as if the sources were also buried at the receiver locations. There are still some challenges that need to be addressed in the virtual source method, such as limited acquisition aperture and energy coming from the overburden. We demonstrate that up-down wavefield separation can substantially improve the quality of virtual source data. First, it allows us to eliminate artifacts associated with the limited acquisition aperture typically used in practice. Second, it allows us to reconstruct a new optimized response in the absence of downgoing reflections and multiples from the overburden. These improvements are illustrated on a synthetic data set of a complex layered model modeled after the Fahud field in Oman, and on ocean-bottom seismic data acquired in the Mars field in the deepwater Gulf of Mexico.

INTRODUCTION

The virtual source method (Bakulin and Calvert, 2004; 2006) is a technique to image and monitor below complex overburden, without knowledge of overburden velocities or near surface changes. The virtual source method is closely related to seismic interferometry (Derode et al., 2003; Schuster et al., 2004; Snieder, 2004; Wapenaar, 2004; Wapenaar et al., 2005); both of them use crosscorrelation of the recorded wavefields at a given pair of receivers to estimate the Green's function between them. For acquisition geometry with downhole receivers and surface shooting, when we correlate the wavefield recorded by a selected reference receiver with every other receiver and sum the correlated wavefield (correlation gather) over the physical sources, the resultant wavefield represents the data recorded as if there was a physical source at the reference receiver location. Because there is no physical source at the reference receiver location, the method is known as the virtual source method (Bakulin and Calvert, 2004; 2006). In practical applications there are still challenges in the virtual source method that need to be addressed. The goal of this study is to identify these challenges and demonstrate the usefulness of wavefield separation to overcome some of them.

The simplest approach to generate virtual source gathers is to crosscorrelate the total wavefield recorded at the virtual source location with the total wavefield recorded at the receivers (Mehta et al., 2006). Total wavefield refers to the entire seismic recording. The resultant virtual source gather includes all the responses between the virtual source and the receiver, some of which may not be of interest for geophysical applications. The current practice is to correlate the windowed direct arrival in the total wavefield recording at the virtual source with the total wavefield at the receivers (Bakulin and Calvert, 2004; 2006). This approach suppresses some of the unwanted responses, coming from the overburden, as compared to the simplest approach. Neither approaches give the true subsurface response, which is obtained by putting a physical source at the virtual source location, because of two reasons.

According to theory (Derode et al., 2003; Schuster et al., 2004; Snieder, 2004; Wapenaar, 2004; Bakulin and Calvert, 2006; Korneev and Bakulin, 2006), we get the true response between a given pair of receivers by correlating the wavefields recorded at the two receivers and summing the correlated signal over sources that populate a closed surface enclosing the two receivers. For geophysical applications, we cannot have sources all around the receivers, and hence simple crosscorrelation and summation over a subset of sources does not provide the true response. Apart from the spurious events caused by incomplete source aperture, in both approaches we get reflections from the overburden and the free surface, because we record both the upgoing and the downgoing waves at the receivers. These unwanted responses obscure the target reflections.

We attempt to suppress the artifacts caused by incomplete source aperture, and the reflections coming from the overburden and the free surface. We do this by separating the recorded wavefield into upgoing and downgoing waves. Up-down wavefield separation shows promise for improving virtual source data quality by removing the reflections from the overburden and nonphysical events arising because of incomplete source aperture. Similar up-down wavefield separation is done by Snieder et al. (2006a) in a different context applied to structural engineering.
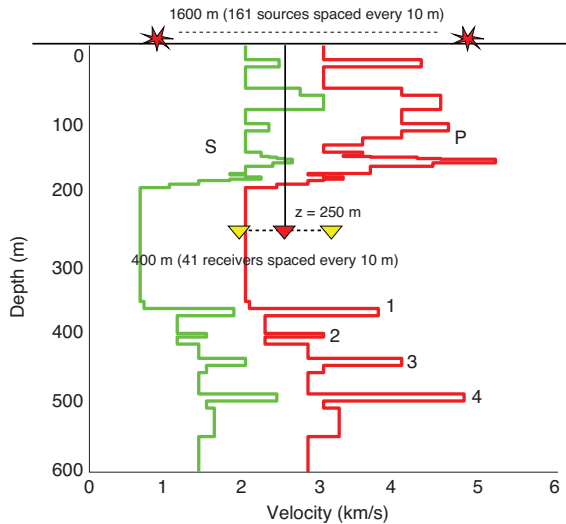

Figure 1. P- and S-wave velocity profiles and the acquisition geometry for synthetic model inspired by Middle East field Fahud. The 161 sources are spaced every 10 m on the surface and 41 receivers are placed on a horizontal well at a depth of 250 m. Receiver spacing is 10 m.

Apart from imaging below complex overburden, virtual source method is also a powerful tool for time-lapse monitoring with permanent receivers. We apply the virtual source method to multicomponent, ocean-bottom cable (OBC) data recorded at the Mars field (Rigzone) with 120 four-component sensors permanently placed on the seafloor. We show in the final section how wavefield separation helps suppress the strong reflection coming from the sea surface, and hence unravels the reflection response of the reservoir. This improves the repeatability for seismic monitoring, by making the response independent of variations in the sea level, sea temperature, source locations, and source signatures.

In the next section, we illustrate the improvement in the virtual source method after incorporating wavefield separation using a synthetic model, followed by an explanation of the need for wavefield separation before crosscorrelating the recordings.

SYNTHETIC MODELING

Let us start by synthetic simulation using a model with vertical profiles of P- and S-wave velocities as shown in Figure 1. The data for this synthetic simulation are generated using reflectivity modeling (Schmidt and Tango, 1986). The density varies between 2100 and 2500 kg/m^3. The acquisition geometry consists of 161 sources (vertical forces) placed on the surface with an interval of 10 m and 41 receivers placed in a horizontal well 250 m deep, with an interval of 10 m. The objective is to create virtual sources along the horizontal well to suppress the distorting effects of the upper near surface (above 200 m), and to get better images of the reservoir layers below. This complex overburden that consists of layers with extremely high-velocity contrasts is typical in the Middle East, and here modeled after the Fahud field in Oman.

If ideal redatuming is performed with seismic interferometry, then the reconstructed response corresponds to buried virtual source at one of the receivers. This response will contain reflections from the overburden layers, as well as free-surface multiples.

Bakulin and Calvert (2006) showed how gating before crosscorrelation can eliminate some of the overburden reflections by making the virtual source radiate predominantly downwards and hence, provides cleaner response from deep target reflectors. Their approach, however, cannot suppress the downgoing reflections and multiples from the free surface and overburden. Here, we set a goal to completely eliminate from the virtual source data all the downgoing reflections and multiples related to the overburden.

Therefore, we benchmark the virtual source data against the ground truth response computed for a new model where all overburden above the well is replaced by a homogeneous half-space with the same velocity structure below the receivers (Figure 1).

We choose receiver 21 (middle receiver) as the virtual source, highlighted in red in Figure 1. This virtual source gather should be equivalent to the response generated by putting a physical source at the location of receiver 21. Figure 2 shows a comparison of the two responses. Figure 2a shows the virtual source gather generated by
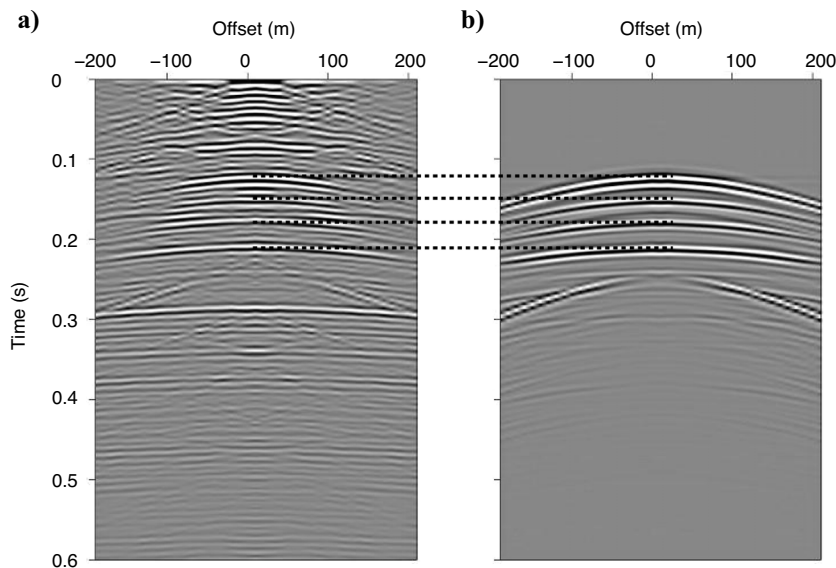

Figure 2. The virtual source gather generated by crosscorrelating the total wavefield at the virtual source (receiver 21) with the total wavefield at the receivers (a), and the shot gather generated by placing a physical source (vertical force) at the virtual source location (receiver 21) and a homogeneous half-space above it (b). In (b), the laterally propagating shear waves have been removed.

crosscorrelating the total wavefield at the virtual source location (receiver 21) with the total wavefield at the receivers. Figure 2b shows the wavefield recorded by the receivers caused by a physical source (vertical force) at the virtual source location, after removing the laterally propagating shear waves. The laterally propagating shear waves are removed by using only the upgoing energy at the receivers. The up-down separation was done by the modeling program during the forward modeling. For the rest of this paper, we will refer to this response as the ground truth response. Apart from the four P-P reflection events, labeled 1 through 4 in Figure 1, that are present in both the cases, there are a lot of other events in the virtual source gather.

For easier comparison, we plot the ground truth response as shown in Figure 3. We see the four P-P reflections labeled 1–4 and also an S-to-P-wave conversion. For further analysis, we restrict ourselves to P-waves only. Figure 4 shows the virtual source gather, plotted in red, on top of the ground truth, plotted in black. As mentioned earlier, apart from the agreement in the reflection events, there are numerous other events in the virtual source gathers. Some of them are of physical nature (overburden-related response) and some are unphysical (artifacts caused by limited source aperture), but both represent unwanted responses in geophysical applications. In the next section, we elaborate on their nature in layered media and demonstrate how wavefield separation can suppress both types of undesired responses.

WAVEFIELD SEPARATION

Before we incorporate wavefield separation in the virtual source method, we demonstrate, using illustrations in Figure 5, the usefulness of wavefield separation to suppress artifacts and overburden response. The figure shows illustrations for a three-layer model to illustrate the effect of incomplete source aperture and reflections coming from the overburden and the free surface. In all the illustrations, the red triangle is the virtual source and the yellow triangle is the receiver. They both are located at depth and the source is excited on the surface. Figure 5a shows the source location that gives a prominent contribution (Snieder et al., 2006b) for a physical arrival between the virtual source and the receivers, as shown by the black arrows. Hence, this source contributes to the true response between the virtual source and the receiver and is referred to as the stationary phase contributor (Snieder et al., 2006b).

If, however, the source is placed as shown in Figure 5b, the virtual source and the receiver will record the wavefield propagating along the red arrows. Snieder et al. (2006b) explains that even though the source gives a stationary phase contribution, crosscorrelation of the two wavefields does not correspond to any physical arrival between them. Hence, this source does not contribute to the true response. Such arrivals contribute to spurious events in the virtual-source gather. Snieder et al. (2006b) also show that if we would have a source below the receivers, as shown in Figure 5c, the waves propagating along the blue arrows will cancel the effect of the waves propagating along the red arrows and hence the spurious event will not be a part of the response. However, for geophysical applications we do not have the luxury to put a source in the subsurface, as shown in the illustration.

To remove these spurious events, we resort to wavefield separation. As shown in Figure 5b, the wavefield propagating along the red arrows, recorded by the virtual source and the receivers is upgoing.

If we restrict the wavefield at the virtual source to be only downgoing, we can suppress these spurious events.

Even though the waves at the virtual source are downgoing, we will get reflections from the overburden and the free surface as shown by the red arrows in Figure 5d. These correspond to physical arrivals and would be a part of the response, if we had a physical source at the virtual source location. We can suppress the effect of these arrivals by restricting the waves at the receivers to be only upgoing. Hence, we get the subsurface response by correlating the downgoing energy at the virtual source location with the upgoing energy at the receivers. The idea is similar to Noah's deconvolution (Riley and Claerbout, 1976), an approach to generate seismograms in the absence of the free surface effects by deconvolving the upgoing waves with the downgoing waves. If such a wavefield separation is achievable without distortions, it may represent an improvement over the current practice of time windowing the direct arrival at the virtual source location and correlating that with the total wavefield at the receivers (Bakulin and Calvert, 2006).
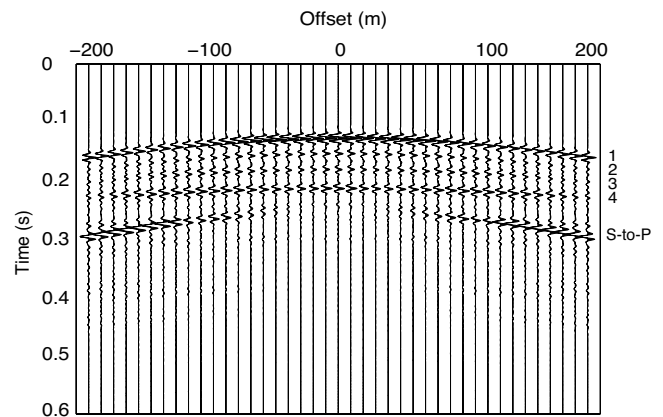
Figure 3. Ground truth response generated by putting a physical source (vertical force) at the virtual source location (receiver 21). The laterally propagating shear waves have been removed.
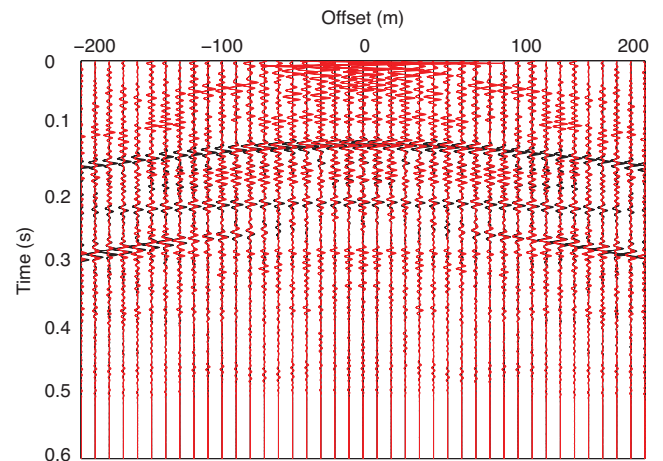
Figure 4. The virtual source gather generated by crosscorrelating the total wavefield at the virtual source (receiver 21) with the total wavefield at the receivers (red lines) and the ground truth response (black lines).

Windowing in time

As discussed above, the current practice involves correlation of direct arrival windowed in the total wavefield at the virtual source with the total wavefield at the receivers. Figure 6 shows the virtual source gather (in red) generated by the current practice. The windowed direct arrival is obtained by placing a time gate of 40 ms around the direct arrival. The reflections are preserved. As compared to Figure 4 a lot of spurious events are, however, suppressed. The suppression is caused by restricting the energy at the virtual source location to be mostly downgoing P-wave energy (in the form of direct arrival). Time windowing the direct arrival, thus, improves the virtual source gather, although a better wavefield separation approach is to decompose the wavefield into upgoing and downgoing waves.

Up-down separation

As demonstrated by the illustrations in Figure 5, we get the desired subsurface response by correlating the downgoing energy at the virtual source location with the upgoing energy at the receivers. Instead of time windowing, we separate the wavefields into upgoing and downgoing waves and use those for correlation. Figure 7 shows the virtual source gather (in red) generated by correlating the downgoing waves at the virtual source with the upgoing waves at the receivers. The spurious events are suppressed and the virtual source gather is practically on top of the ground truth response. Hence, wavefield separation is indeed a promising tool for suppressing the downgoing reflections and multiples in the process of generating the virtual source gather.

The up-down separation and time windowing can also be combined to generate the virtual source gather as shown in Figure 8. This virtual source gather is generated by correlating the direct arrival
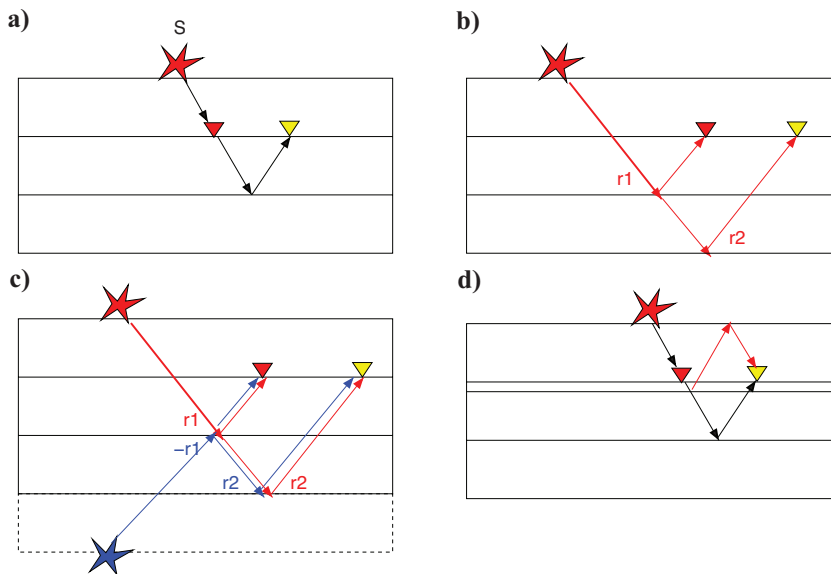
windowed in the downgoing waves at the virtual source location with the upgoing waves at the receivers. For this synthetic model it shows an improvement over Figure 7.

For field data, this improvement will become prominent once we separate the recorded wavefield into upgoing and downgoing waves. In case of horizontally layered media, wavefield separation for field data can be done by dual-sensor summation (e.g., Robinson, 1999). According to dual-sensor summation, if we have hydrophone (H) and vertical component geophone (Z) recording at the same sensor location, the sum H + Z gives the upgoing energy and the difference H − Z gives the downgoing energy. Before we apply this to field data, we compare the exact downgoing and upgoing waves, for our synthetic model with the H − Z and H + Z approximations respectively.

Figure 9 shows the exact downgoing waves for the raw data (black) and H − Z (red). Similarly, Figure 10 shows the exact upgoing waves for the raw data (black) and H + Z (red). The wavefields are practically identical, suggesting that, despite being strictly valid for zero-offset data in horizontally layered media, dual-sensor summation technique provides a reasonable separation of the wavefield into upgoing and downgoing waves at all offsets at hand.

FIELD EXAMPLE: REDATUMING OCEAN-BOTTOM SEISMIC AT MARS FIELD

We demonstrate the improvement in the virtual source gathers, because of wavefield separation, using the data recorded for seismic monitoring of the Mars field located in the Gulf of Mexico. Figure 11 shows an illustration of the acquisition geometry. The geometry consists of 364 air guns fired (spaced every 25 m) near the sea surface with 120 four-component sensors (spaced every 50 m) permanently placed on the seafloor at 1-km depth. Sea level, water velocity, and shot locations change slightly between repeat acquisitions, even though receivers remain fixed on the seabed. This creates a problem for seismic monitoring aimed to detect small time shifts and amplitude changes related to field depletion. The virtual source method allows us to redatum OBC data to the seabed without knowing any of these factors. Redatumed data should correspond to fixed (virtual) source and fixed receiver and exhibit greatly improved repeatability between surveys. This was shown by Bakulin and Calvert (2006) for synthetic and real data of repeated VSP acquired over time-varying overburden.

For the synthetic model, we demonstrated the improvement in the virtual source gathers by up-down separation. For the Mars field data, we use the dual-sensor summation technique for the separation of the wavefield into upgoing and downgoing waves. We use these separate upgoing and downgoing waves to generate the improved virtual source gathers.

We choose receiver 60 (middle receiver) as the virtual source and sum the correlation gather over all the sources. Figure 12a shows the virtual source gather, for the hydrophone component, generated by correlating the total wavefield recorded at the virtual source location with the total

Figure 5. Illustration explaining the need for wavefield separation. S is the source and r1 and r2 are the reflection coefficients at the interfaces. (a) The source location that gives the stationary phase contribution for a physical arrival between the virtual source and the receiver. (b) The source location that gives stationary phase contribution for a nonphysical arrival between the virtual source and the receiver. (c) The hypothetical source below the receivers, which if present, would cancel the effect of the nonphysical arrival. (d) The presence of reflections from the overburden and/or the free-surface multiples.

wavefield at the receivers. The most prominent reflection we see is the reflection from the sea surface, labeled as *?multiple?* in the figure. The arrow with the *?primary?* is the location where we expect the strongest true reflection from the subsurface. Hence, even for a simple overburden, correlating the total wavefields gives a virtual source gather dominated by the reflection from the overburden (sea surface).

Before summing and differencing the hydrophone and the vertical geophone, it is essential to calibrate the vertical geophone to the hydrophone, because there could be coupling variations and/or amplifier-gain differences in the hydrophone and the vertical component geophone. The calibration of the vertical geophone to the hydrophone is done by aligning the first arrivals for hydrophone and vertical component geophone and determining a scalar per vertical geophone using the upgoing energy that arrives immediately after the direct arrival (Jiao et al., 1998). Thereafter, using the calibrated hydrophone and the vertical component geophone recording and the

Figure 8. The virtual source gather generated by crosscorrelating the direct arrival windowed in the downgoing waves at the virtual source (receiver 21) with the upgoing waves at the receivers (red lines) and the ground truth response (black lines).
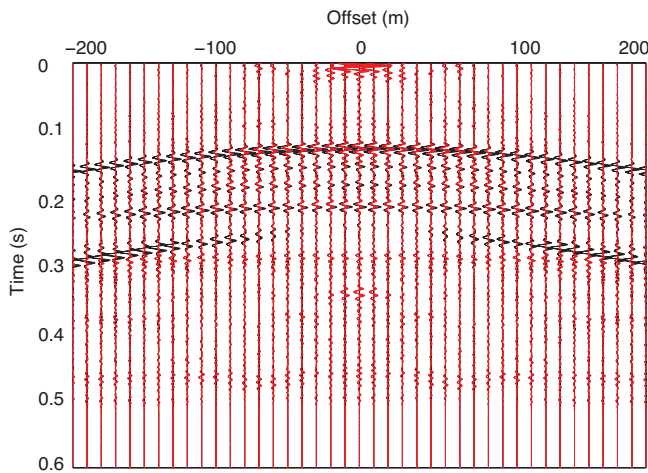

Figure 6. The virtual source gather generated by crosscorrelating the windowed direct arrival at the virtual source (receiver 21) with the total wavefield at the receivers (red lines) and the ground truth response (black lines).

Figure 9. Comparison of the exact downgoing waves (black lines) with the $H - Z$ approximation (red lines).
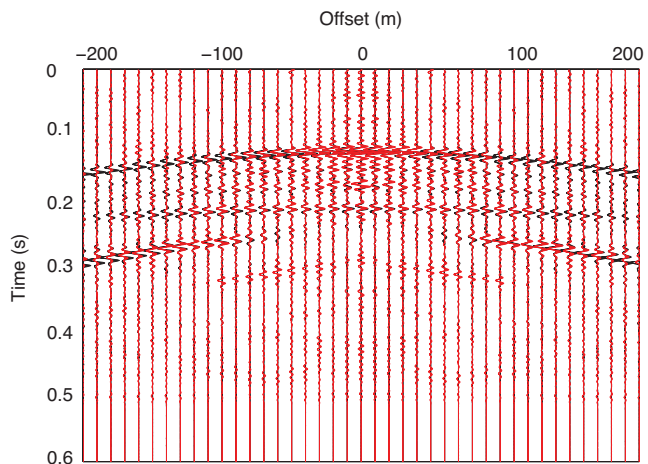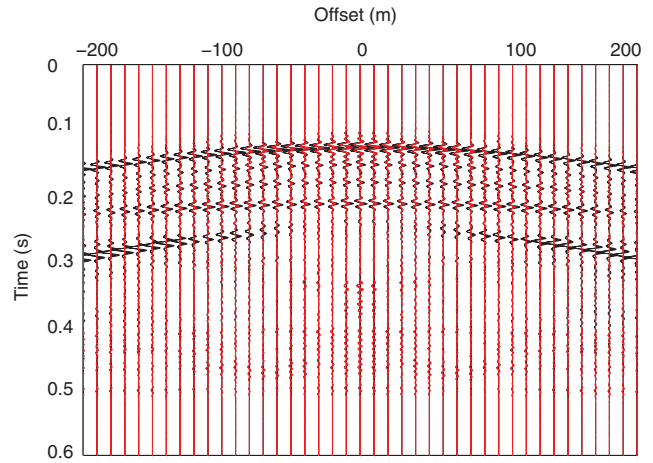

Figure 7. The virtual source gather generated by crosscorrelating the downgoing waves at the virtual source (receiver 21) with the upgoing waves at the receivers (red lines) and the ground truth response (black lines).
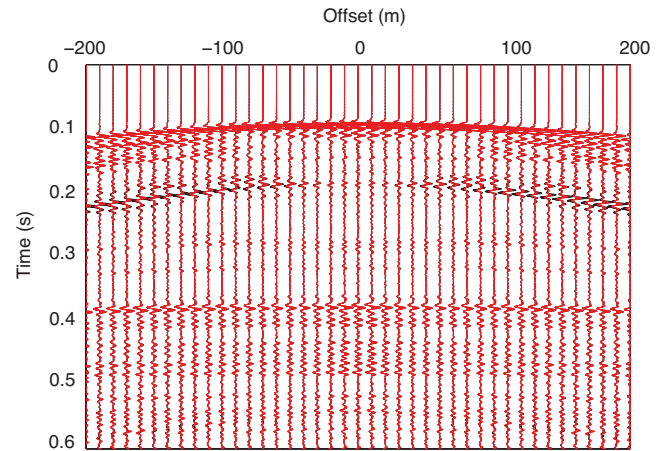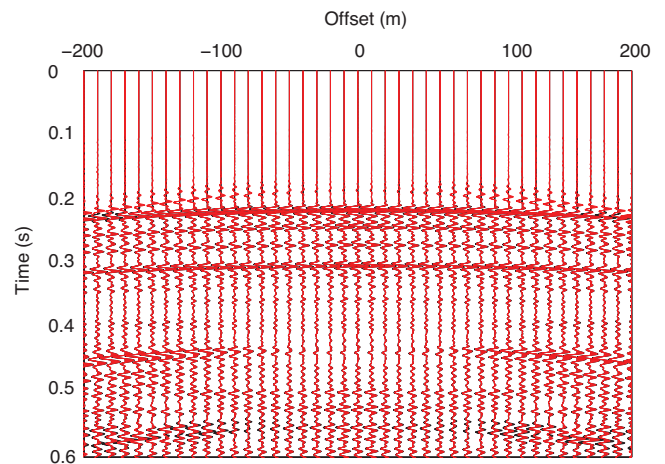

Figure 10. Comparison of the exact upgoing waves (black lines) with the $H + Z$ approximation (red lines).

dual-sensor summation technique, we separate the upgoing and downgoing waves at all receivers. If instead of correlating the total wavefields, we correlate the downgoing waves at the virtual source with the upgoing waves at the receivers, we obtain virtual source gather shown in Figure 12b. The free-surface multiple is suppressed (highlighted by the arrow and *?multiple?*). The reflections from the deeper subsurface are now visible and the strongest one is highlighted by an arrow and labeled as *?primary?*. Even though the reflections from the subsurface are visible, the virtual source gather is still noisy.

Figure 13a shows the virtual source gather obtained by the current practice (Bakulin and Calvert, 2004; 2006): correlating the windowed direct arrival in the total wavefield at the virtual source location with the total wavefield at the receivers. The windowed direct arrival is obtained by placing a time gate of 400 ms around the direct arrival. Correlating the time-windowed direct arrival makes the virtual source gather cleaner, but the strongest reflection is still the free-surface multiple (labeled as *?multiple?* To further improve the virtu-
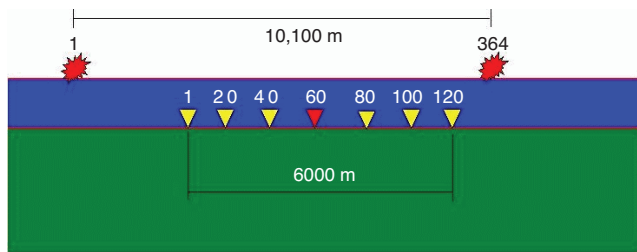

Figure 11. Illustration showing the geometry of the Mars field OBC data acquisition. There are 120 receivers spaced every 50 m on the seafloor and 364 air guns (spaced every 25 m) are fired near the sea surface. Water depth is 1 km.

al source gather quality, we combine the up-down separation and the time-windowing approach. As shown in Figure 13b, if we correlate the direct arrival windowed in the downgoing waves at the virtual source location with the upgoing waves at the receiver, the virtual source gather is cleaner and the true subsurface response (highlighted by the arrow and labeled as *?primary?*) is clearly visible in the absence of the free-surface multiples. The free-surface multiple (labeled as *?multiple?* is attenuated because we use only the upgoing energy at the receivers. The early-time reflections are crisper in Figure 13b than in Figure 13a because we excluded any upgoing energy that may have been left in the windowing approach. The near-offset jitter in Figure 13b around 3 to 4 s is the result of the wave scattering near the soft sea bottom. These scattered and mode-converted waves are sensed by the vertical component and show up in the virtual source gather when we include the vertical component for up-down wavefield separation.

We conclude that the combination of wavefield separation and gating produces the best response out of all (Figure 13b) as predicted by synthetic modeling. Although wavefield separation restricts the radiation pattern of the virtual source to be strictly downward, additional gating makes the radiation pattern of the virtual source predominantly longitudinal and, thus, improves signal-to-noise ratio by eliminating unwanted shear-wave energy from the virtual source. This unwanted late energy may be used to generate virtual shear sources (Bakulin and Calvert, 2005).

Dual-sensor summation is strictly valid for zero-offset data over horizontally layered media. Therefore, in many practical instances of large offsets or complex (2D and 3D) overburdens, it may fail to deliver separated wavefields with undistorted phase required for virtual source generation. In cases such as borehole observations below near surface, an alternative approach can be attempted to unravel improved reflection response of the subsurface. First, one can generate two virtual source (*VS*) data sets using the current practice, i.e., correlating the direct arrival windowed in the total wavefield at the virtual source with the total wavefield at the receivers, both for the hydrophone (VS_H) and vertical component geophone (VS_Z) separately, and then extract the upgoing waves ($VS_H + VS_Z$) for downhole survey using dual-sensor summation. Figure 14b, generated by such an alternate approach, reveals a gather similar in quality to our best response Figure 14a (same as Figure 13b). In Figure 14b, there are, however, distortions in early times and near the direct arrival because of windowing in the total wavefield, instead of windowing in the downgoing waves. As shown before, wavefield separation in the process of generating the virtual source gathers indeed gives the desired subsurface response. This alternative approach with wavefield separation after generating the virtual source data, however, also gives reasonable reflection response and can be improved further by suitable combination of 3-C sources and 4-C geophones, i.e., by doing elastic (vector) virtual source.

The up-down wavefield separation applied to the virtual source method suppresses the downgoing reflections and multiples from the overburden as shown in the Figure 5. There are, however, waves that propagate downwards from the virtual
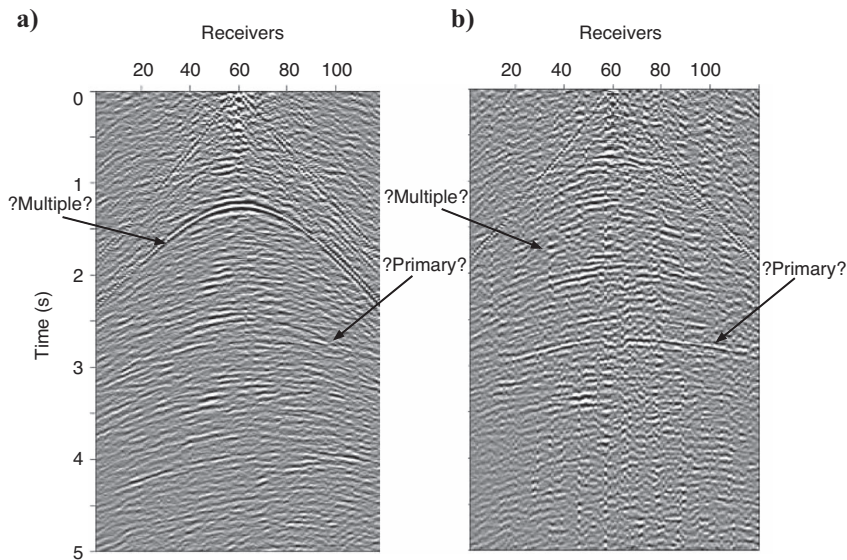

Figure 12. Virtual source gathers generated with receiver 60 as the virtual source. (a) The virtual source gather generated by crosscorrelating the total wavefields at both the virtual source and receiver locations. (b) The virtual source gather generated by crosscorrelating the downgoing waves at the virtual source location with the upgoing waves at the receivers. *Multiple* refers to the reflection from the free-surface (overburden) and *primary* refers to the reflection from the subsurface. The *???* refers to the absence of the reflection event.
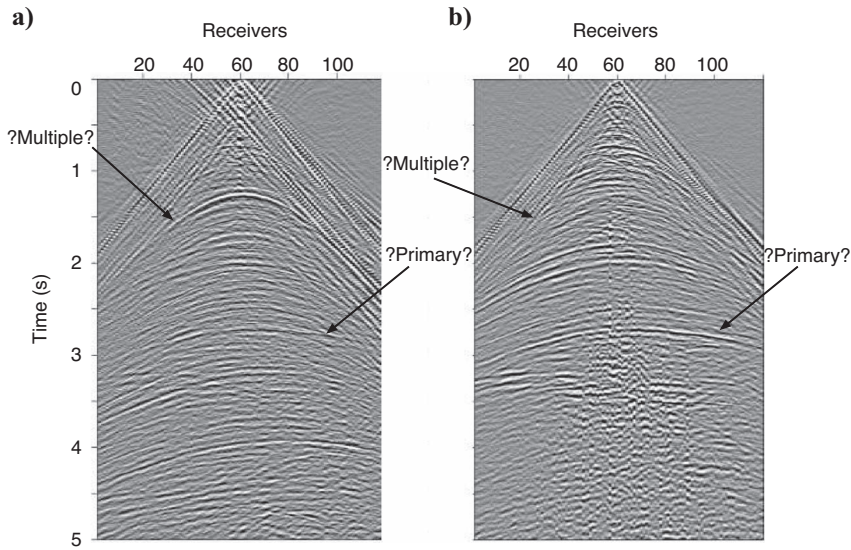
Figure 13. Virtual source gathers generated with receiver 60 as the virtual source. (a) The virtual source gather generated by crosscorrelating the direct arrival windowed in the total wavefield at the virtual source with the total wavefield at the receiver locations. (b) The virtual source gather generated by crosscorrelating the direct arrival windowed in the downgoing waves at the virtual source location with the upgoing waves at the receivers. *Multiple* refers to the reflection from the free surface (overburden) and *primary* refers to the reflection from the subsurface. The *???* refers to the absence of the reflection event.
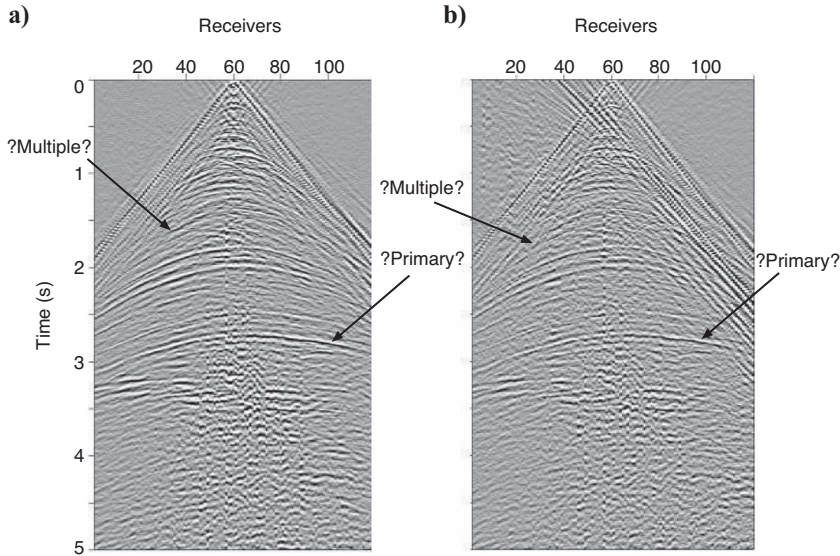

Figure 14. Virtual source gathers generated with receiver 60 as the virtual source. (a) The virtual source gather generated by crosscorrelating the direct arrival windowed in the downgoing waves at the virtual source location with the upgoing waves at the receivers. (b) The virtual source gather generated by summing the virtual source gathers generated for hydrophone and vertical component geophone. Each is generated separately by crosscorrelating the direct arrival windowed in the total wavefield at the virtual source location with the total wavefield at the receivers. *Multiple* refers to the reflection from the free surface (overburden) and *primary* refers to the reflection from the subsurface. The *???* refers to the absence of the reflection event.

source, reflect from the subsurface, propagate through the overburden above the receivers, reflect back into the subsurface, and are sensed by the receivers as upgoing waves. Such events exist in the virtual source data, even after applying wavefield separation. Wavefield separation, hence, suppresses the overburden-related primaries and common-leg multiples. The overburden-related multiples that are downgoing at the virtual source and upgoing at the receivers, however, still exists even after applying wavefield separation.

CONCLUSIONS

The virtual source method can be improved to get mainly the reflection response from the deeper subsurface by using wavefield separation combined with gating. Instead of correlating total wavefields as suggested by theory, in practice it is more beneficial to correlate downgoing waves at the virtual source with the upgoing waves at the receivers. In addition, time windowing or gating of the downgoing response further improves the signal-to-noise ratio.

Synthetic modeling in layered media inspired by the Fahud field in Oman reveals the nature of these improvements. Selecting upgoing waves at the receivers eliminate the reflections from the overburden and free surface. Using downgoing waves at the virtual source restricts the radiation pattern of the virtual sources to downward direction only and hence, suppresses the spurious events caused by incomplete acquisition aperture. Combination of the two provides us with a new optimized response in the absence of downgoing reflections and multiples from the overburden. Additional gating of the downgoing response allows for restricting the virtual source radiation pattern to predominantly P-waves and avoids contamination by shear energy. A field data example confirms that a combination of wavefield separation and gating leads to a greatly improved signal-to-noise ratio on virtual source data and, thus, a cleaner reflection response of target horizons.

REFERENCES

Bakulin, A., and R. Calvert, 2004, Virtual source: New method for imaging and 4D below complex overburden: 74th Annual Meeting, SEG, Expanded Abstracts, 2477–2480.
———, 2005, Virtual shear source: A new method for shear-wave seismic surveys: 75th Annual Meeting, SEG, Expanded Abstracts, 2633–2636.
———, 2006, The virtual source method: Theory and case study: Geophysics, **71**, no. 4, SI139–SI150.
Derode, A., E. Lacrose, M. Campillo, and M. Fink, 2003, How to estimate the Green's function for a heterogeneous medium between two passive sensors?: Application to acoustic waves: Applied Physics Letters, **83**, 3054–3056.
Jiao, J., S. Trickett, and B. Link, 1998, Robust summation of dual-sensor ocean-bottom cable data: 68th Annual Meeting, SEG, Expanded Abstracts, 1421–1424.
Korneev, V., and A. Bakulin, 2006, On the fundamentals of the virtual source method: Geophysics, **71**, no. 3, A13–A17.
Mehta, K., R. Snieder, R. Calvert, and J. Sheiman, 2006, Virtual source gathers and attenuation of free-surface multiples using OBC data: Implementation issues and a case study: 76th Annual Meeting, SEG, Expanded Abstracts, 2669–2673.
Rigzone official web site, "Project: Mars," http://www.rigzone.com/data/projects/project_detail.asp?project_id=27, accessed December 1, 2006.

Riley, D. C., and J. F. Claerbout, 1976, 2-D multiple reflections: Geophysics, **41**, 592–620.
Robinson, E. A., 1999, Seismic inversion and deconvolution, Part B: Dual-sensor technology: Elsevier Science Publishing Co., Inc.
Schmidt, H., and G. Tango, 1986, Efficient global matrix approach to the computation of synthetic seismograms: Geophysical Journal of Royal Astronomical Society, **84**, 331–359.
Schuster, G. T., J. Yu, J. Sheng, and J. Rickett, 2004, Interferometric/daylight seismic imaging: Geophysics Journal International, **157**, 838–852.
Snieder, R., 2004, Extracting the Green's function from the correlation of coda waves: A derivation based on stationary phase: Physics Review E, **69**, 046610.
Snieder, R., J. Sheiman, and R. Calvert, 2006a, Equivalence of the virtual source method and wavefield deconvolution in seismic interferometry: Physics Review E, **73**, 066620.
Snieder, R., K. Wapenaar, and K. Larner, 2006b, Spurious multiples in interferometric imaging of primaries: Geophysics, **71**, no. 4, SI65–SI78.
Wapenaar, K., 2004, Retrieving the elastodynamic Green's function of an arbitrary inhomogeneous medium by cross-correlation: Physics Review Letters, **93**, 254301.
Wapenaar, K., J. Fokkema, and R. Snieder, 2005, Retrieving the Green's function by cross-correlation: A comparison of approaches: Journal of Acoustical Society of America, **118**, 2783–2786.